Extra-framework aluminium species in hydrated faujasite zeolite as investigated by two-dimensional solid-state NMR spectroscopy and theoretical calculations

ARTICLE *in* PHYSICAL CHEMISTRY CHEMICAL PHYSICS · APRIL 2010

Impact Factor: 4.49 · DOI: 10.1039/b915401a · Source: PubMed

8 AUTHORS, INCLUDING:

Shenhui Li
Chinese Academy of Sciences
27 PUBLICATIONS **514** CITATIONS
SEE PROFILE

Anmin Zheng
Chinese Academy of Sciences
104 PUBLICATIONS **1,636** CITATIONS
SEE PROFILE

Yongchao Su
Massachusetts Institute of Technology
38 PUBLICATIONS **749** CITATIONS
SEE PROFILE

Zhiwu Yu
Wuhan National High Magnetic Field Center
18 PUBLICATIONS **252** CITATIONS
SEE PROFILE

Extra-framework aluminium species in hydrated faujasite zeolite as investigated by two-dimensional solid-state NMR spectroscopy and theoretical calculations†

Shenhui Li, Anmin Zheng, Yongchao Su, Hanjun Fang, Wanling Shen, Zhiwu Yu, Lei Chen and Feng Deng*

Received 28th July 2009, Accepted 28th January 2010
First published as an Advance Article on the web 24th February 2010
DOI: 10.1039/b915401a

Extra-framework aluminium (EFAL) species in hydrated dealuminated HY zeolite were thoroughly investigated by various two-dimensional solid-state NMR techniques as well as density functional theoretical calculations. ^{27}Al MQ MAS NMR experiments demonstrated that five-coordinated and four-coordinated extra-framework aluminium subsequently disappeared with the increase of water loading, and the quadrupole interaction of each aluminium species decreased gradually during the hydration process. ^{1}H double quantum MAS NMR revealed that the EFAL species in the hydrated zeolite consisted of three components: a hydroxyl AlOH group, and two types of water molecule (rigid and mobile water). ^{1}H–^{27}Al LG-CP HETCOR experiments indicated that both the extra-framework and the framework Al atoms were in close proximity to the rigid water in the fully rehydrated zeolite. The experimental results were further confirmed by DFT theoretical calculations. Moreover, theoretical calculation results further demonstrated that the EFAL species in the hydrated zeolite consisted of the three components and the calculated ^{1}H NMR chemical shift for each component agreed well with our NMR observations. It is the rigid water that connects the extra-framework aluminium with the four-coordinated framework aluminium through strong hydrogen bonds.

1. Introduction

Faujasite zeolite is a catalyst widely used for catalytic cracking, hydrocracking and isomerization in the petroleum refinery process. As is well-known, a hydrothermal or calcination treatment of faujasite zeolite usually causes the dealumination of its framework, forming extra-framework aluminium (EFAL) species, which can considerably enhance the catalytic activity of the zeolite.[1–3] Several forms of the EFAL species have been proposed in the literature: cationic species such as Al^{3+}, AlO^{+}, $Al(OH)_2^{+}$ and $AlOH^{2+}$, and neutral or polymeric species such as AlOOH, $Al(OH)_3$ and Al_2O_3.[4] However, it is difficult to discriminate various EFAL species in dehydrated zeolite sample by ^{27}Al NMR directly because of the existence of strong quadrupolar interactions that come from the asymmetry of the local environment of EFAL species.[5,6] While with the presence of water molecule, the EFAL species acting as Lewis acid sites are likely coordinated with the water to form more stable EFAL species in dealuminated zeolites, which may considerably improve the symmetry around EFAL species and thus decreases the quadrupolar interaction. Therefore, hydrated zeolite samples were usually used to detect the ^{27}Al NMR signals of various aluminium species.[7,8] It was found that the rehydration of dealuminated zeolites began with the adsorption of molecular water on the Lewis acid site, and then on the Brønsted acid site.[7,8]

The EFAL species in dehydrated or hydrated zeolites have been studied by ^{1}H, ^{27}Al as well as ^{1}H/^{27}Al TRAnsfer of Populations in DOuble Resonance (TRAPDOR) Magic Angle Spinning (MAS) NMR spectroscopy previously.[5,6,8–15] ^{1}H MAS NMR can give the direct information about various hydroxyl groups such as AlOH, SiOH and SiOHAl hydroxyl groups in zeolites,[12,15] while ^{1}H/^{27}Al TRAPDOR MAS NMR experiments can distinguish whether the hydroxyl groups are strongly coupled with aluminium nuclei or not.[10] Meanwhile, the ^{27}Al NMR can discriminate the framework Al from the extra-framework Al in zeolites according to their isotropic chemical shifts.[13,14] However, one-dimensional solid-state NMR can give us only limited information about the detailed structure of EFAL species in zeolites.

Nevertheless, with the development of two-dimensional MAS NMR spectroscopy, several powerful methods for studying the detailed structure of EFAL species in zeolites are available. ^{27}Al Multiple-Quantum (MQ) MAS NMR[16,17] was not only used to determine the real line shape of aluminium signals in ^{27}Al MAS NMR, but also used to study the coordination state of various aluminium species present in the zeolites. Two-dimensional (2D) ^{1}H double-quantum (DQ) MAS NMR experiment has been proved to be a very useful method for probing proton–proton spatial proximities

State Key Laboratory of Magnetic Resonance and Atomic and Molecular Physics, Wuhan Center for Magnetic Resonance, Wuhan Institute of Physics and Mathematics, the Chinese Academy of Sciences, Wuhan 430071, China. E-mail: dengf@wipm.ac.cn; Fax: +86-27-87199291

† Electronic supplementary information (ESI) available: Details of ^{2}H NMR experiments. See DOI: 10.1039/b915401a

in various solid materials.[18,19] Furthermore, the correlation information between two nearby hetero-nuclear atoms can be established through space or through bonds by HETCOR[20] or HMQC[21] MAS NMR experiments.

As is well known, quantum chemical calculations can be widely used to predict the structure, acidity and catalytic performance of zeolites.[22,23] Many works have been done to investigate the EFAL species in zeolites by employing theoretical calculations.[24–30] Benco *et al.*[24] performed *ab initio* molecular dynamics calculations on some hydrated aluminium hydroxide inside zeolite channels. Zhidomirov *et al.*[25] also investigated the dialuminium oxide clusters, as models of EFAL and Lewis acid sites in zeolites through theoretical calculations. Ruiz *et al.*[26] studied the relative stability of tetracoordinated, pentacoordinated and hexacoordinated aluminium hydroxyl species, which could be considered as models of EFAL. Mota *et al.*[27,28] found that the extra-framework aluminium species were coordinated with the oxygen atoms nearby the framework aluminium in USY zeolite through DFT calculation.

The combination of solid state NMR and theoretical calculations has been successfully employed to determine the framework structure[31,32] and the existence of EFAL species[33] in various zeolites. In our recent work,[33] by employing ^{1}H DQ MAS NMR spectroscopy, the detailed spatial proximities between the Brønsted and Lewis acid sites were obtained, and ^{13}C NMR of adsorbed 2-^{13}C-acetone demonstrated that the spatial proximity (or synergy) could result in a remarkable increase in the acid strength of dealuminated HY zeolite. In combination with DFT theoretical calculations, the detailed structure of EFAL species (acting as Lewis acid) and the mechanism of Brønsted/Lewis acid synergy were revealed for the first time. Extra-framework $Al(OH)_3$ and $AlOH^{2+}$ species in the supercage, as well as $AlOH^{2+}$ species in the sodalite cage, are the preferred Lewis acid sites in the dealuminated HY zeolite. However, the nature of these EFAL species in the presence of water molecules is still uncertain. In addition, we also explored the spatial proximities and the synergy of Brønsted and Lewis acid sites in H–Y zeolites treated with various dealumination methods (calcination, steam, and acid treatments) and at different levels of dealumination by means of ^{1}H, ^{27}Al, ^{29}Si and ^{13}C MAS NMR in conjunction with ^{1}H DQ MAS NMR techniques.[34] It was found that the extra-framework AlOH species (Lewis acid sites) are always in close proximity to the bridging AlOHSi hydroxyls (Brønsted acid sites) on the framework of dealuminated H–Y zeolites prepared by calcination and steam treatments, indicating the presence of a Brønsted/Lewis acid synergy effect. Whereas such an effect is absent in acid-treated H–Y zeolites, as also confirmed by ^{13}C CP/MAS NMR of adsorbed 2-^{13}C-acetone.[34]

In this work, several two-dimensional experiments, including ^{27}Al MQ MAS NMR, ^{1}H double quantum MAS NMR as well as ^{1}H–^{27}Al LG-CP HETCOR, were employed to study the property and detailed structure of EFAL species in hydrated dealuminated HY zeolite. In addition, theoretical calculations were applied as well to confirm the proposed structure of EFAL species.

2. Experimental section

2.1 Sample preparation

Zeolite Na–Y with a Si/Al ratio of 2.8 was exchanged in a 1.0 mol L^{-1} aqueous solution of NH_4Cl at 353 K for 4 h several times. The obtained sample was washed with distilled water until no chloride ions could be detected any more. The obtained NH_4–Y was dried in air at 353 K overnight. Dealuminated HY zeolite was prepared as follows: the NH_4Y sample was placed in a quartz crucible in a tube furnace and calcined at 773 K in air for 4 h (the temperature was raised from room temperature to 773 K at a rate of 3 K min^{-1}). The Si/Al ratio of the dealuminated HY was determined to be 3.5 by ^{29}Si MAS NMR spectroscopy,[34] indicating that each unit cell consisted of 141.5 Si atoms, 42.7 framework Al atoms and 7.8 extra-framework Al atoms in the dealuminated sample.

For the sample dehydration and the subsequent water adsorption, about 0.2 g dealuminated HY sample was placed in a glass tube that was connected to a vacuum line. The temperature was raised at a rate of 1 K min^{-1} and the sample was kept at 673 K under a pressure below 10^{-3} Pa over 8 h and then cooled. A known amount of water was introduced and frozen on the activated catalyst with liquid N_2. Then the glass tube was flame sealed. Prior to NMR measurements, the sealed sample was transferred into a ZrO_2 rotor (sealed by a Kel-F cap) under a dry nitrogen atmosphere in a glovebox.

2.2 Solid-state NMR spectroscopy

^{1}H and ^{27}Al NMR experiments were carried out on a Varian Infinityplus-400 spectrometer equipped with a triple-resonance 5 mm probe at resonance frequencies of 400.12 and 104.26 MHz respectively. For the ^{1}H spin-echo and DQ MAS NMR experiments, a 10 kHz sample spinning rate and a 5 s recycle delay were used. ^{1}H DQ coherences were excited and reconverted with the POST-C7 pulse sequence.[35] 20 μs t_1 increment interval, 128 t_1 increments, and 64 scans accumulations for each t_1 increment were used in the ^{1}H DQ MAS NMR experiments. ^{27}Al MQ MAS spectra were recorded with the pulse sequence proposed by Amoureux *et al.*[36] 480 scans were accumulated and the recycling delay was set to 1.0 s. Hyper-complex method was used in the 2D ^{27}Al MQ MAS data acquisition and processing. The MAS spin rate was 10 kHz in ^{27}Al single-pulse and MQ MAS experiments. ^{1}H–^{27}Al Lee-Goldburg Cross Polarization (LG-CP) HETCOR experiment (PMLG[37,38] was employed in the evolution period) was performed to suppress the spin diffusion and chemical exchange during the ^{1}H evolution period according to the previous work.[39,40] 800 μs of LG-CP contact time and 48 t_1 increments were used in the HETCOR experiment. 256 scans were accumulated for each t_1 increment and the spinning speed was set to 6 kHz. The ^{1}H and ^{27}Al chemical shifts were referenced to tetramethylsilane (TMS) and 1 mol L^{-1} aqueous $Al(NO_3)_3$ solution, respectively.

2.3 Computational details

Fig. 1a shows the structure of faujasite zeolite, which consists of supercages, sodalite cages and double 6-ring prisms. The supercage has a free aperture of 0.74 nm, while the sodalite

cage, linked together by the double 6-ring prisms, has a 6-ring opening of 0.26 nm. A 24 T cluster model (1/8 unit cell of HY zeolite, shown in Fig. 1b) containing six framework aluminium atoms and one EFAL was selected to represent the real structure of the HY zeolite. The Si/Al ratio of this cluster model was 3.0, which is similar to the experimental value. Such 24 T cluster model was formed by two interconnected 12-ring systems in the supercage. The structure parameters adopted during the calculations were extracted from the crystallographic structural data of HY.[41] The terminal hydrogen atoms are located at a Si–H distance of 1.47 Å from the corresponding silicon, orienting along the bond direction to the next oxygen atom.

$Al(OH)_3$ was taken into account as the initial structure of EFAL species,[33] and three water molecules (corresponding to 24 water molecules per unit cell) were added to represent the EFAL species in the hydrated HY zeolite, in which stable six-coordinated extra-framework aluminium species $[Al(OH)_3(H_2O)_3]$ was formed. During the geometry optimization process, all the O–Al–OH–Si–O in the 12-ring as well as the EFAL species and H_2O were allowed to relax, while the remained atoms were kept fixed, which could avoid losing the unique structure of faujasite zeolite in the full optimization. The structure optimizations were performed by density functional theory (DFT) method at B3LYP/6-31g(d) level. On the basis of the optimized structure, the ^1H NMR chemical shifts were calculated using the gauge-independent atomic orbital (GIAO) approach at the B3LYP/6-311g(d,p) level. The calculated ^1H NMR chemical shifts were referenced to CH_3OH whose experimental chemical shift for the hydroxyl proton is 0.02 ppm in gas state.[42] All the calculations were performed using Gaussian03 program package.[43]

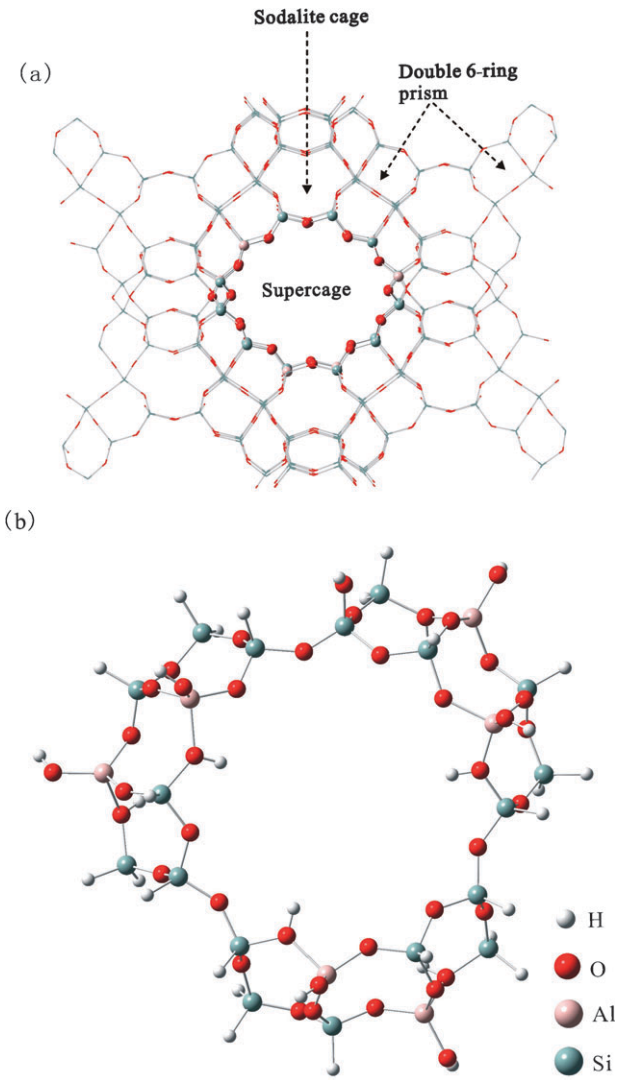

Fig. 1 The structure of HY zeolite (a) and the selected 24 T cluster as the computational model (b).

3. Results and discussion

3.1 ^{27}Al MAS and MQ MAS NMR

^{27}Al MAS NMR has been established as an efficient probe to determine the coordination and the local structure of specific aluminium species in zeolites since each ^{27}Al site can be readily resolved based on their distinctly different chemical shifts. Fig. 2 shows the ^{27}Al MAS NMR spectra of the dealuminated HY as a function of water loadings. Obviously, the hydration process has a significant effect on the ^{27}Al MAS spectra. In general, three broad peaks at around 60, 30 and 0 ppm can be observed in the ^{27}Al MAS spectra of the hydrated samples. The 60 ppm signal results from four-coordinated framework A1, while the peak centered at around 30 ppm arises from five-coordinated extra-framework Al, and the resonance at 0 ppm is associated with six-coordinated extra-framework Al.[8,9] Since ^{27}Al MQ MAS NMR can provide a more resolved pattern compared with ^{27}Al MAS NMR after averaging out the second-order quadrupole interaction, it was employed to investigate the variation of the chemical environment of each

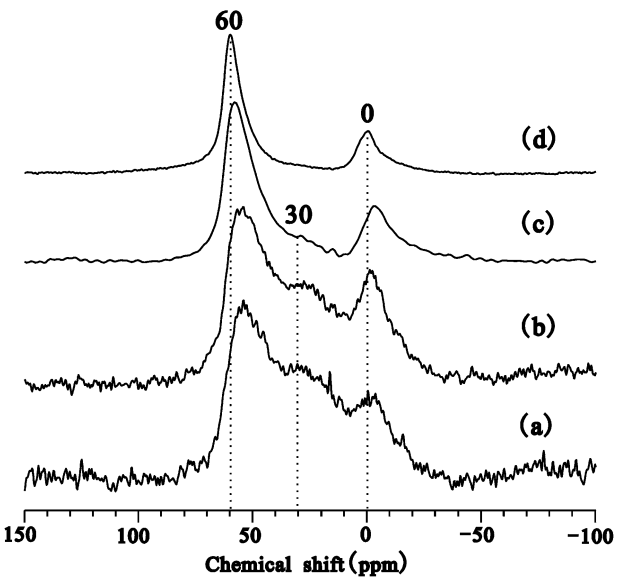

Fig. 2 ^{27}Al MAS NMR spectra of dealuminated HY zeolite with different water loadings: (a) 3 H_2O/u.c., (b) 10 H_2O/u.c., (c) 30 H_2O/u.c. and (d) 200 H_2O/u.c. (full hydration).

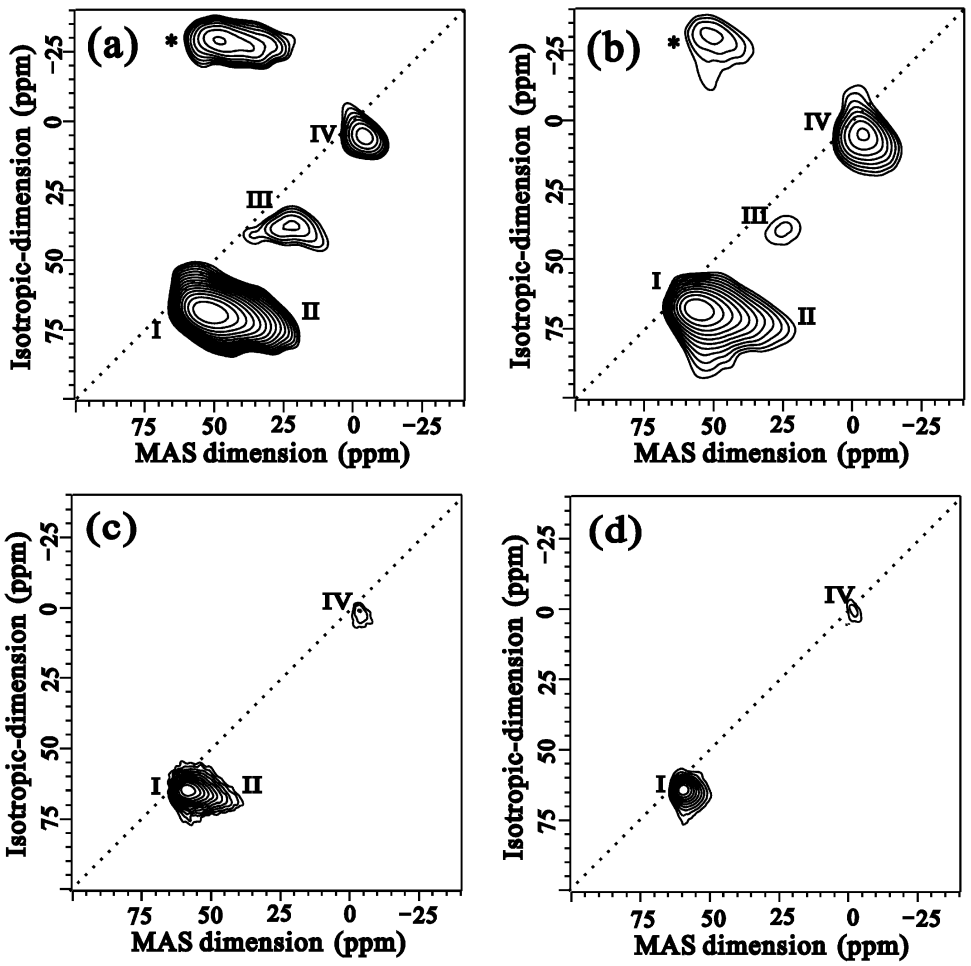

Fig. 3 ^{27}Al MQ MAS NMR spectra of dealuminated HY zeolite with different water loadings: (a) 3 H_2O/u.c., (b) 10 H_2O/u.c., (c) 30 H_2O/u.c. and (d) 200 H_2O/u.c. (full hydration). Four aluminium species, marked as I, II, III and IV, can be assigned to four-coordinated framework Al, four-coordinated EFAL, five-coordinated EFAL and six-coordinated EFAL, respectively.

Al species during the hydration process. Fig. 3 shows the ^{27}Al MQ MAS spectra of dealuminated HY zeolites with different water loadings in which the dotted lines indicated the scaling used along F_{iso}.[44] At least four aluminium species (marked as I, II, III and IV) are distinguished, which can be assigned to four-coordinated framework Al, four-coordinated extra-framework Al, five-coordinated extra-framework Al and six-coordinated extra-framework Al, respectively.[45–47] It can be seen from Fig. 3 that the five-coordinated EFAL and four-coordinated EFAL gradually disappear at the high water loading. The isotropic chemical shift δ_{iso} as well as the second-order quadrupolar interaction parameter P_Q of each aluminium species can be deduced from the position of signals in the 2D MQ spectrum by the following formula:[48]

$$\delta_{iso} = (17\delta_{F1} + 10\delta_{F2})/27 \quad (1)$$

$$P_Q = C_{QCC}\sqrt{1+\frac{\eta^2}{3}} = \left(\frac{17}{162000}\nu_L^2(\delta_{F1}-\delta_{F2})\right)^{1/2} \quad (2)$$

δ_{iso} represents the isotropic chemical shift, δ_1 and δ_2 are the centers of gravity of the signals in the F_1 and F_2 dimension respectively, ν_L is the Larmor frequency, and C_{QCC} and η are the quadrupole coupling constant and the asymmetry parameter, respectively. Table 1 displays the δ_{iso} and the corresponding

Table 1 Isotropic chemical shift δ_{iso} and second-order quadrupolar interaction parameter P_Q of each aluminium species in dealuminated HY zeolite as a function of water loading

	Peak parameters as determined by ^{27}Al MQ MAS NMR							
	I		II		III		IV	
Water loading	δ_{iso} (ppm)	P_Q/MHz	δ_{iso} (ppm)	P_Q/MHz	δ_{iso} (ppm)	P_Q/MHz	δ_{iso} (ppm)	P_Q/MHz
3 H_2O/u.c.	61.8	4.5	57.3	7.5	31.3	4.3	1.2	3.5
10 H_2O/u.c.	63.3	3.8	59.9	6.9	33.9	4.1	1.5	3.4
30 H_2O/u.c.	62.2	2.7	60.2	4.8			1.6	2.5
200 H_2O/u.c.	62.6	2.2					−0.3	1.5

P_Q of each Al species at different hydration states, from which it is obvious that the δ_{iso} of each aluminium species changed slightly, whereas the P_Q of each species considerably decreases as the increase of water loading.

Based on the experimental results, it can be expected that as water molecules were loaded on the dealuminated zeolite, water molecules were tightly adsorbed on both Lewis and Brønsted acid sites. As suggested by Hunger *et al.*,[7] hydration led to deprotonation of the Brønsted acid site (SiOHAl) and protonation of adsorbed water molecules, forming hydroxonium ions in the zeolite. This was accompanied by an improvement on the symmetry around the Al atoms, and thus a decrease in C_{QCC} and the line widths as well. Eventually, narrow ^{27}Al NMR signals could be observed. For the extra-framework Al species (Lewis acid sites), similar behavior may occur in the hydration process. The previous ^{1}H/^{27}Al TRAPDOR, ^{27}Al spin-echo and ^{27}Al MQ MAS NMR experiments[5,6,10,49,50] demonstrated that the EFAL species in several dehydrated zeolites had a C_{QCC} much larger than 10 MHz. For our HY zeolites with low water loadings (shown in Fig. 3a–b), parts of water molecules were tightly adsorbed on the Lewis acid site, resulting in a decrease in P_Q of the EFAL species in the form of four-, five-, or six-coordinations. When more water molecules were loaded on the zeolite, the EFAL species were further coordinated to adsorbed water molecules, leading to the disappearance of five- and four-coordinated EFAL species, and the formation of more stable six-coordinated EFAL structure: $Al(OH)_m(H_2O)_n$ ($m + n = 6$). As the water loading increases to 200 H_2O/u.c., all of the EFAL species became six-coordinated and the P_Q of EFAL species was decreased to 1.5 MHz due to the full water coordination (see Table 1 and Fig. 3d).

3.2 ^{1}H MAS and DQ-MAS NMR

Fig. 4 displays the ^{1}H NMR spectra of dealuminated HY as a function of water loadings. As shown in Fig. 4a and b, ^{1}H MAS NMR spectra of dealuminated HY with low water loadings (3 and 10 H_2O/u.c.) consist of six well-resolved signals at 6.7, 5.0, 4.3, 2.8, 2.2 and 1.0 ppm. The peaks at 5.0 and 4.3 ppm are assigned to the bridging OH groups (Brønsted acid site) in the sodalite cage and the faujasite cage, respectively.[51,52] The resonances at 2.8 and 1.0 ppm are due to the EFAL species in the faujasite and sodalite cage, respectively, based on the previous ^{1}H DQ MAS NMR experiments.[51,52] The peak at 2.2 ppm arises from non-acidic SiOH groups at framework defects in amorphous parts of the sample.[7,15,51]

According to the literature,[6,7] the peak appearing at 6.7 ppm was assigned to the water adsorbed on the Lewis acid sites. As the water loading was increased to 30 H_2O/u.c, a new signal at *ca.* 9.5 ppm due to adsorbed water molecule in the form of $Al(H_2O)_6^{3+}$ could be clearly distinguished in Fig. 4c,[7] while with the water loadings up to 200 H_2O/u.c. (full hydration), due to the fast chemical exchange, a major peak at *ca.* 5.4 ppm is predominant in the ^{1}H MAS NMR spectrum (shown in Fig. 4d).

Two-dimensional ^{1}H DQ MAS NMR experiment is a powerful method for probing proton–proton proximities in various solid materials.[18,19] Since the DQ coherences observed

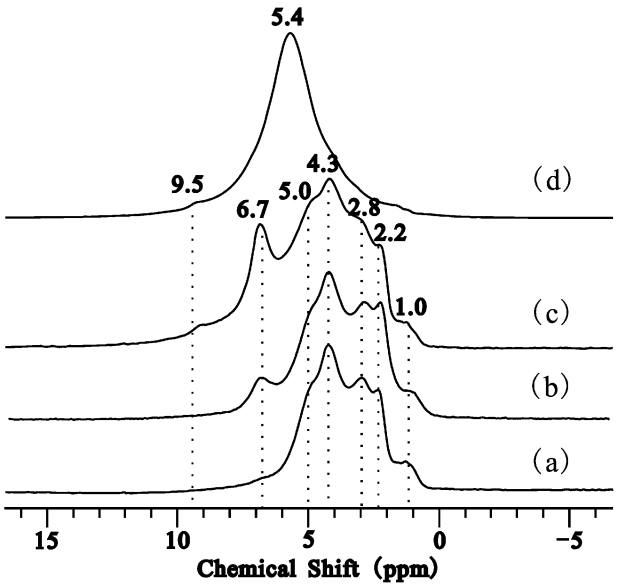

Fig. 4 ^{1}H MAS NMR spectra of dealuminated HY zeolite with different water loadings: (a) 3 H_2O/u.c., (b) 10 H_2O/u.c., (c) 30 H_2O/u.c. and (d) 200 H_2O/u.c. (full hydration).

are strongly dependent on the internuclear distance, the presence of a signal in the ^{1}H DQ MAS spectrum indicates that two protons are in close proximity (< 5 Å). Peaks that occur along the diagonal (ω, 2ω) are autocorrelation peaks resulting from the dipolar interaction of protons with the same chemical shift. While pairs of off-diagonal peaks at (ω_a, $\omega_a + \omega_b$) and (ω_b, $\omega_a + \omega_b$) correspond to correlations between two protons with different chemical shifts. Here, we employed the ^{1}H DQ-MAS NMR to study the detailed spatial proximities among various protons in the hydrated zeolite.

Fig. 5 shows the ^{1}H DQ-MAS NMR spectrum of dealuminated HY zeolite with a water loading of 10 H_2O/u.c. Five autocorrelation peaks can be clearly observed. The two autocorrelation peaks at (4.3, 8.6) and (5.0, 10.0) ppm indicates the spatial proximities between Brønsted acid sites in the supercage and the sodalite cage, respectively. The third autocorrelation peak at (2.2, 4.4) ppm results from the formation of silanol nests during the dealumination process, while the fourth autocorrelation peak at (2.8, 5.6) ppm is due to either the EFAL species containing more than one hydroxyl group such as $Al(OH)_3$ or EFAL species such as $AlOH^{2+}$ in close proximity. The appearance of the fifth autocorrelation peak at (6.7, 13.4) ppm is due to water molecules adsorbed on Lewis acid sites. The off-diagonal peak pair at (1.0, 6.0) and (5.0, 6.0) ppm suggests the spatial proximity between the extra-framework AlOH group (Lewis acid site) and the bridging hydroxyl group (Brønsted acid sites) in the sodalite cage. The off-diagonal peak pair at (2.8, 7.1) and (4.3, 7.1) ppm confirms the spatial proximity between the Lewis and the Brønsted acid sites in the supercage. The weak off-diagonal peak at (4.3, 5.3 = 4.3 + 1.0) ppm suggests the spatial correlation between the Brønsted acid site in the supercage and the Lewis acid site in the sodalite cage. Apart from the above-mentioned correlation peaks, cross-correlation peaks pair at (2.8, 9.5) and (6.7, 9.5) ppm that is associated with the SQ (single quantum)

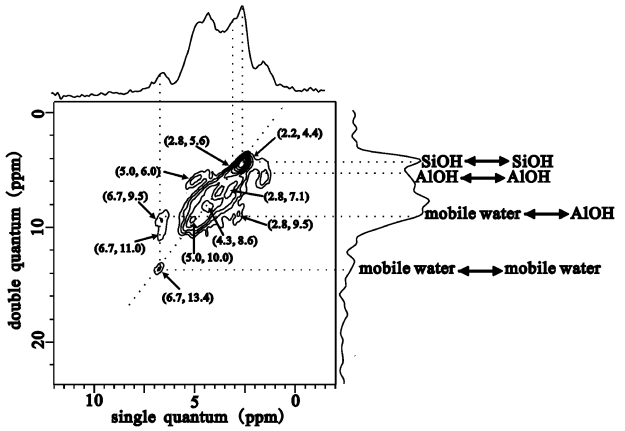

Fig. 5 ^{1}H DQ MAS NMR spectrum of dealuminated HY zeolite with a water loading of 10 H_2O/u.c.

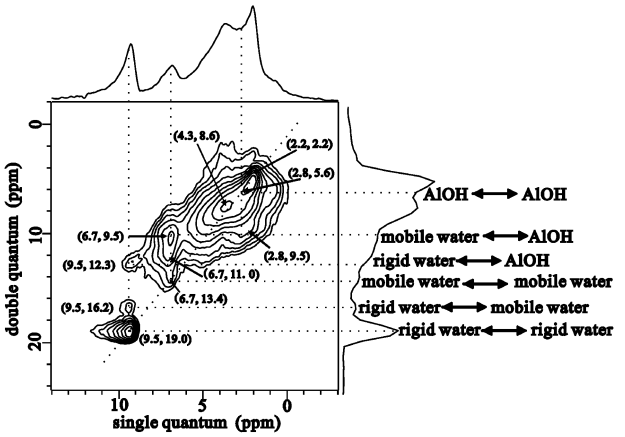

Fig. 6 ^{1}H DQ MAS NMR spectrum of dealuminated HY zeolite with a water loading of 30 H_2O/u.c.

signals at 2.8 and 6.7 ppm can be discerned in Fig. 5, being indicative of the spatial proximity between the adsorbed water molecules and the hydroxyl group of EFAL species. In addition, another weak off-diagonal correlation peak at (6.7, 11.0 = 6.7 + 4.3) ppm is also observable, implying the spatial proximity between the adsorbed water and the Brønsted acid site. Interestingly, the adsorbed water molecules (giving rise to the signal at 6.7 ppm) are in spatial proximity with both the Lewis and the Brønsted acid sites.

With the water loading up to 30 H_2O/u.c., as shown in Fig. 6, the presence of a new autocorrelation peak at (9.5, 19.0) ppm and the large ^{1}H chemical shift of the signal imply the existence of another type of water molecule having strong hydrogen bonds in the hydrated zeolite, while the appearance of off-diagonal peak at (9.5, 16.2 = 9.5 + 6.7) ppm suggests that the two different types of water are in close proximity to one another in the EFAL species. The cross-correlation peak at (9.5, 12.3 = 9.5 + 2.8) ppm and the cross-correlation peaks pair at (6.7, 9.5) and (2.8, 9.5) ppm further confirm the spatial proximity between the extra-framework AlOH hydroxyl group and the two different types of water molecules in the partially hydrated zeolite. Based on the ^{1}H DQ MAS NMR experimental results, we conclude that the extra-framework AlOH groups and two types of water molecules are in close proximity to one another, which means that the EFAL species in the partially hydrated dealuminated HY zeolite consists of three components: AlOH hydroxyl group and two different types of water molecule. The two diagonal peaks at (6.7, 13.4) and (9.5, 19.0) ppm could be mainly ascribed to the intra-molecular autocorrelation between adjacent protons in two different types of water, respectively, whose distances are normally around 1.5–1.6 Å. The contribution of the inter-molecular auto-correlation between the same type water molecules to the two diagonal peaks is negligible, due to the large H–H distance (usually 2.7–5.2 Å as determined by structure optimization, see the following). It is noteworthy that the relative peak intensity of the 6.7 ppm signal is much stronger than that of the 9.5 ppm signal in the ^{1}H MAS NMR spectra (see Fig. 4c), whereas the autocorrelation peak intensity of the former ((6.7, 13.4) ppm) is much weaker than that of the latter ((9.5, 19.0) ppm) in the ^{1}H DQ MAS NMR spectrum (see Fig. 6). Since in the ^{1}H DQMAS NMR experiment, DQ coherences observed are strongly dependent on the dipolar couplings, which are affected by the ^{1}H–^{1}H distance as well as molecular motion,[53,54] it can be concluded that the water molecules associated with the signal at 6.7 ppm are much more mobile than those associated with the signal at 9.5 ppm. Therefore, we can assign the ^{1}H NMR signal at 6.7 and 9.5 ppm to the mobile water and rigid water in the EFAL species, respectively. The existence of the mobile water and rigid water is also confirmed by ^{2}H NMR (see the ESI†). It is likely the formation of strong hydrogen bonds between the rigid water and the nearby oxygen atoms in the surrounding environments that results in the slow motion of water molecules. In addition, as shown in Fig. 6, the diagonal peak of the 4.3 ppm signal became broader as the increase of water loading. It can be inferred that some of the Brønsted acid sites were complexed with water molecules, resulting in the larger chemical shift distribution of the signal in the ^{1}H DQ MAS NMR spectrum.

Fig. 7 shows the ^{1}H DQ MAS NMR spectrum of fully hydrated dealuminated HY, in which only four auto-correlation peaks can be clearly resolved. In comparison with Fig. 6, all the off-diagonal peaks as well as the diagonal peak at (6.7, 13.4) ppm disappear, while the autocorrelation peak at (9.5, 19.0) ppm still remains in Fig. 7. The result indicates again that the water molecules in the EFAL species corresponding to the signal at 9.5 ppm are relatively rigid, while the other type of water molecules corresponding to the peak at 6.7 ppm are relatively mobile. The disappearance of all the off-diagonal peaks under the full hydration condition is due to the fast proton exchange among the various proton species, which remarkably reduces the dipolar couplings between them. Here, the ^{1}H DQ MAS NMR functions as a dipolar filter, only the correlations from strongly coupled spin pairs survive.

3.3 ^{1}H–^{27}Al LG-CP HETCOR experiment

In order to have a better insight into the natures of EFAL species in the hydrated samples, direct information about the proton–aluminium connectivity in the hydrated dealuminated HY is desirable. Fig. 8 shows the CP ^{1}H–^{27}Al PMLG

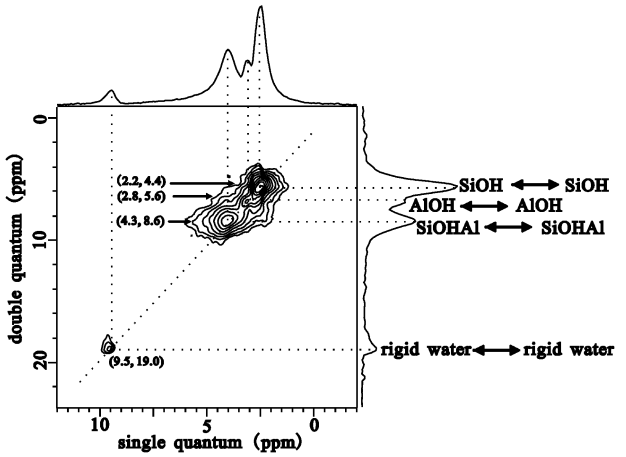

Fig. 7 ^{1}H DQ MAS NMR spectrum of dealuminated HY zeolite with a water loading of 200 H_2O/u.c. (full hydration).

decoupled correlation spectrum of dealuminated HY after full hydration. During the evolution period, PMLG decoupling technique was applied to restrain the spin diffusion and proton exchange.[34] Obviously, the four-coordinated framework Al (at *ca.* 60 ppm) exhibits correlations with the Brønsted acidic proton (4.3 ppm) as well as the rigid water (9.5 ppm), whereas the six-coordinated EFAL species (at *ca.* 0 ppm) shows correlations with the AlOH group (2.8 ppm) of EFAL species and the rigid water (9.5 ppm). The result is consistent with our ^{1}H DQ MAS NMR observation. The LG-CP HETCOR experiments reveal an interesting phenomenon that both the four-coordinated framework Al and the six-coordinated extra-framework Al species are strongly coupled with the rigid water molecules, being indicative of the spatial proximity between the framework aluminium and the extra-framework aluminium species *via* the rigid water. This experimental result will be further discussed by theoretical calculations.

3.4 DFT calculation

Theoretical calculations were carried out to investigate the EFAL species in the hydrated HY zeolite. The B3LYP/6-31g(d) optimized structures for the octahedral EFAL species $[Al(OH)_3(H_2O)_3]$ in the hydrated HY zeolite are displayed in Fig. 9. As the EFAL species $Al(OH)_3$ is spatially connected with the framework, the proton in the Brønsted acid site is transferred to the oxygen atom of one of the AlOH hydroxyl groups in the EFAL species, forming $[Al(OH)_2(H_2O)_4]^+$. Strong hydrogen bonds between the EFAL species and the oxygen atoms nearby the framework Al can be distinguished, resulting in the formation of rigid water in the EFAL species (see Fig. 9), which is consistent with our experimental ^{1}H DQ MAS NMR results. It is the rigid water that connects the extra-framework aluminium with the four-coordinated framework aluminium, consistent with the above ^{1}H–^{27}Al LG-CP HETCOR experiments. The distances between the protons in the rigid water and the two nearest oxygen atoms in the framework are calculated to be 1.654 and 1.747 Å, while the two O–H bond lengths in the rigid water are elongated to 1.005 and 0.993 Å, respectively. It can be concluded that the strong hydrogen bond results in the slow motion of the rigid water. Apart from the rigid water in the EFAL species, other three mobile water molecules are present. It is noteworthy that one of the mobile water molecules is in spatial proximity with both the Lewis and the Brønsted acid sites. Therefore, our theoretical calculation results are in good agreement with the above experimental observations and demonstrate that the EFAL species in dealuminated zeolite consists of three main parts: AlOH hydroxyl group, mobile water and rigid water.

The ^{1}H NMR chemical shifts of EFAL species ($[Al(OH)_2(H_2O)_4]^+$) were also calculated at the B3LYP/6-311G(d,p) level and are listed in Table 2. The average calculated ^{1}H NMR chemical shifts for rigid water, mobile water and AlOH hydroxyl were 9.4, 5.3 and 1.8 ppm respectively, which are in reasonable agreement with the experimental results (9.5, 6.7 and 2.8 ppm). The agreement between the calculated and the experimental results indicates that the computational

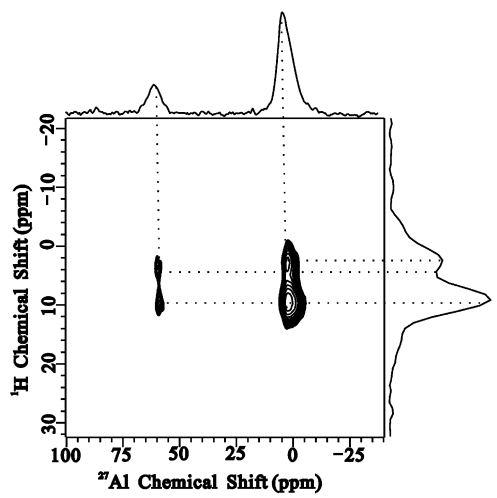

Fig. 8 ^{1}H–^{27}Al LG-CP HETCOR spectrum of the dealuminated HY zeolite after full hydration.

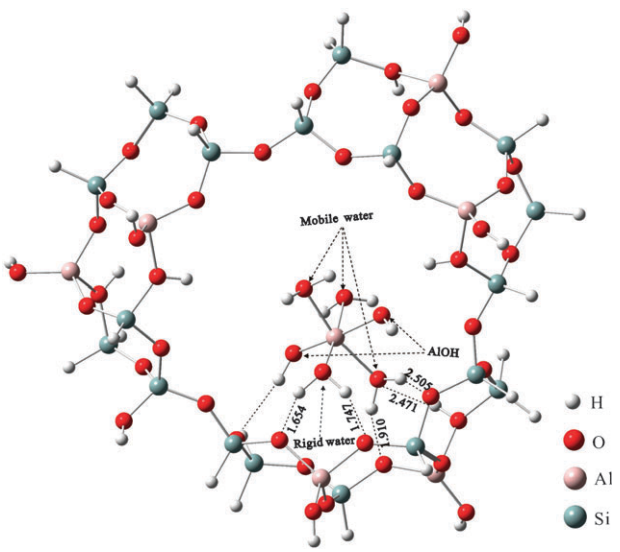

Fig. 9 B3LYP/6-31G(d) optimized structure of the octahedral extra-framework Al species $[Al(OH)_3(H_2O)_3]$ present in the 24 T cluster model of HY zeolite.

Table 2 The calculated ^{1}H NMR chemical shifts of rigid water, mobile water and AlOH hydroxyl. (The corresponding experimental values are also included)

	Rigid water	Mobile water	AlOH
Calcd	10.1, 8.7	8.1, 4.5, 3.7, 6.3, 3.9, 5.5	2.2, 1.3
Avg	9.4	5.3	1.8
Exptl	9.5	6.7	2.7

models are reliable to represent the real structure of the EFAL species present in the hydrated zeolite.

4. Conclusion

The detailed structure of the EFAL species in hydrated dealuminated HY zeolite was investigated by two-dimensional solid state NMR spectroscopy as well as density functional theoretical calculation. The ^{27}Al MQ MAS NMR experiments demonstrated that as the water loaded on the dealuminated HY zeolite, water molecules adsorbed on the Lewis and Brønsted acid sites subsequently, and the five-coordinated and four-coordinated extra-framework Al disappeared consequently, and the P_Q of each aluminium species decreased during the hydration process. The ^{1}H double quantum MAS NMR experiment revealed that the EFAL species in hydrated zeolite consisted of three components: AlOH hydroxyl group, and two types of water molecule (rigid water and mobile water). The ^{1}H–^{27}Al LG-CP HETCOR experiments indicated that the extra-framework aluminium was spatially connected to the framework aluminium *via* the rigid water molecule. Theoretical calculations further confirmed the proposed structure of EFAL species present in the hydrated dealuminated HY zeolite, *i.e.*, the calculated ^{1}H chemical shift of each component in the EFAL species agreed well with our NMR observations.

Acknowledgements

We are grateful for the support of the National Natural Science Foundation of China (Grants 20933009, 20773159, and 20703058). The authors are grateful to Shanghai Supercomputer Center (SSC, China) for their supports in computing facilities.

Notes and References

1 R. A. Beyerlein, G. B. McVicker, L. N. Yacullo and J. J. Ziemiak, *J. Phys. Chem.*, 1988, **92**, 1967–1970.
2 J. R. Sohn, S. J. DeCanio, P. O. Fritz and J. H. Lunsford, *J. Phys. Chem.*, 1986, **90**, 4847–4851.
3 S. J. DeCanio, J. R. Sohn, P. O. Fritz and J. H. Lunsford, *J. Catal.*, 1986, **101**, 132–141.
4 R. D. Shannon, K. H. Gardner, R. H. Staley, G. Bergeret, P. Gallezot and A. Auroux, *J. Phys. Chem.*, 1985, **89**, 4778–4788.
5 H. M. Kao and G. P. Grey, *J. Phys. Chem.*, 1996, **100**, 5105–5117.
6 D. Feng, Y. Yue and C. H. Ye, *Solid State Nucl. Magn. Reson.*, 1998, **10**, 151–160.
7 M. Hunger, D. Freude and H. Pfeifer, *J. Chem. Soc., Faraday Trans.*, 1991, **87**, 657–662.
8 F. Deng, Y. R. Du, C. H. Ye, J. Z. Wang, T. T. Ding and H. X. Li, *J. Phys. Chem.*, 1995, **99**, 15208–15214.
9 F. Deng, Y. Yue and C. H. Ye, *J. Phys. Chem. B*, 1998, **102**, 5252–5256.
10 C. P. Grey and A. J. Vega, *J. Am. Chem. Soc.*, 1995, **117**, 8232–8242.
11 D. Ma, F. Deng, R. Q. Fu, X. W. Dan and X. H. Bao, *J. Phys. Chem. B*, 2001, **105**, 1770–1779.
12 M. Hunger, *Solid State Nucl. Magn. Reson.*, 1996, **6**, 1–29.
13 L. B. Alemany, *Appl. Magn. Reson.*, 1993, **4**, 179–201.
14 M. E. Smith, *Appl. Magn. Reson.*, 1993, **4**, 1–64.
15 H. Pfeifer, D. Freude and M. Hunger, *Zeolites*, 1985, **5**, 274–286.
16 L. Frydman and J. S. Harwood, *J. Am. Chem. Soc.*, 1995, **117**, 5367–5368.
17 A. Medek, J. S. Harwood and L. Frydman, *J. Am. Chem. Soc.*, 1995, **117**, 12779–12787.
18 S. P. Brown, *Prog. Nucl. Magn. Reson. Spectrosc.*, 2007, **50**, 199–251.
19 S. P. Brown and H. W. Spiess, *Chem. Rev.*, 2001, **101**, 4125–4155.
20 P. Caravatti, L. Braunschweiler and R. R. Ernst, *Chem. Phys. Lett.*, 1983, **100**, 305–310.
21 D. Massiot, F. Fayon, B. Alonso, J. Trebosc and J.-P. Amoureux, *J. Magn. Reson.*, 2003, **164**, 160–164.
22 J. B. Nicholas, *Top. Catal.*, 1997, **4**, 157–171.
23 C. J. Rhodes, *Prog. React. Kinet. Mech.*, 2008, **33**, 1–79.
24 L. Benco, T. Demuth, J. Hafner, F. Hutschka and H. Toulhoat, *J. Catal.*, 2002, **209**, 480–488.
25 G. M. Zhidomirov, A. L. Yakovlev, M. A. Milov, N. A. Kachurovskaya and I. V. Yudanov, *Catal. Today*, 1999, **51**, 397–410.
26 J. M. Ruiz, M. H. McAdon and J. M. Garces, *J. Phys. Chem. B*, 1997, **101**, 1733–1744.
27 D. L. Bhering, A. Ramirez-Solis and C. J. A. Mota, *J. Phys. Chem. B*, 2003, **107**, 4342–4347.
28 C. J. A. Mota, D. L. Bhering and N. Rosenbach, *Angew. Chem., Int. Ed.*, 2004, **43**, 3050–3053.
29 U. Fleischer, W. Kutzelnigg, A. Bleiber and J. Sauer, *J. Am. Chem. Soc.*, 1993, **115**, 7833–7838.
30 O. Lisboa, M. Sanchez and F. Ruette, *J. Mol. Catal. A: Chem.*, 2008, **294**, 93–101.
31 S. Sklenak, J. Dedecek, C. Li, B. Wichterlova, V. Gabova, M. Sierka and J. Sauer, *Phys. Chem. Chem. Phys.*, 2009, **11**, 1237–1247.
32 S. Cadars, D. H. Brouwer and B. F. Chmelka, *Phys. Chem. Chem. Phys.*, 2009, **11**, 1825–1837.
33 S. Li, A. Zheng, Y. Su, H. Zhang, L. Chen, J. Yang, C. Ye and F. Deng, *J. Am. Chem. Soc.*, 2007, **129**, 11161–11171.
34 S. Li, S.-J. Huang, W. Shen, H. Zhang, H. Fang, A. Zheng, S.-B. Liu and F. Deng, *J. Phys. Chem. C*, 2008, **112**, 14486–14494.
35 M. Hohwy, H. J. Jakobsen, M. Eden, M. H. Levitt and N. C. Nielsen, *J. Chem. Phys.*, 1998, **108**, 2686–2694.
36 J. P. Amoureux, C. Fernandez and S. Steuernagel, *J. Magn. Reson., Ser. A*, 1996, **123**, 116–118.
37 M. Lee and W. I. Goldburg, *Phys. Rev.*, 1965, **140**, A1261–A1271.
38 E. Vinogradov, P. K. Madhu and S. Vega, *Chem. Phys. Lett.*, 1999, **314**, 443–450.
39 B. J. van Rossum, H. Forster and H. J. M. de Groot, *J. Magn. Reson.*, 1997, **124**, 516–519.
40 X. J. Ai, F. Deng, J. X. Dong, W. Hu, H. Xu and C. H. Ye, *Solid State Nucl. Magn. Reson.*, 2004, **25**, 216–226.
41 J. A. Hriljac, M. M. Eddy, A. K. Cheetham, J. A. Donohue and G. J. Ray, *J. Solid State Chem.*, 1993, **106**, 66–72.
42 L. Smith, A. K. Cheetham, R. E. Morris, L. Marchese, J. M. Thomas, P. A. Wright and J. Chen, *Science*, 1996, **271**, 799.
43 M. J. Frisch, G. W. Trucks, H. B. Schlegel, G. E. Scuseria, M. A. Robb, J. R. Cheeseman, J. A. Montgomery, Jr., T. Vreven, K. N. Kudin, J. C. Burant, J. M. Millam, S. S. Lyengar, J. Tomasi, V. Barone, B. Mennucci, M. Cossi, G. Scalmani, N. Rega, G. A. Petersson, H. Nakatsuji, M. Hada, M. Ehara, K. Toyota, R. Fukuda, J. Hasegawa, M. Ishida, T. Nakajima, Y. Honda, O. Kitao, H. Nakai, M. Klene, X. Li, J. E. Knox, H. P. Hratchian, J. B. Cross, C. Adamo, J. Jaramillo, R. Gomperts, R. E. Stratmann, O. Yazyev, A. J. Austin, R. Camml, C. Pomelli, J. W. Ochterski, P. Y. Ayala, K. Morokuma, G. A. Voth, P. Salvador, J. J. Dannenberg, V. G. Zakrzewski, S. Dapprich, A. D. Daniels, M. C. Strain, O. Farkas, D. K. Malick, A. D. Rabuck, K. Raghavachari, J. B. Foresman, J. V. Ortiz, Q. Cui, A. G. Baboul, S. Clifford, J. Cioslowski, B. B. Stefanov, G. Liu, A. Liashenko, P. Piskorz, I. Komaromi, R. L. Martin, D. J. Fox, T. Keith, M. A. Al-Laham,

C. Y. Peng, A. Nanayakkara, M. Challacombe, P. M. W. Gill, B. Johnson, W. Chen, M. W. Wong, C. Gonzalez and J. A. Pople, *GAUSSIAN 03 (Revision B.05)*, Gaussian Inc., Pittsburgh, PA, 2003.
44 J. Jiao, J. Kanellopoulos, W. Wang, S. S. Ray, H. Foerster, D. Freude and M. Hunger, *Phys. Chem. Chem. Phys.*, 2005, **7**, 3221–3226.
45 J. X. Chen, T. H. Chen, N. J. Guan and J. Z. Wang, *Catal. Today*, 2004, **93–95**, 627–630.
46 D. Ma, X. W. Han, S. J. Xie, X. H. Bao, H. B. Hu and S. C. F. Au-Yeung, *Chem.–Eur. J.*, 2002, **8**, 162–170.
47 J. A. van Bokhoven, D. C. Koningsberger, P. Kunkeler, H. van Bekkum and A. P. M. Kentgens, *J. Am. Chem. Soc.*, 2000, **122**, 12842–12847.
48 G. Engelhardt, A. P. M. Kentgens, H. Koller and A. Samoson, *Solid State Nucl. Magn. Reson.*, 1999, **15**, 171–180.
49 J. Jiao, S. Altwasser, W. Wang, J. Weitkamp and M. Hunger, *J. Phys. Chem. B*, 2004, **108**, 14305–14310.
50 J. Huang, Y. Jiang, V. R. R. Marthala, B. Thomas, E. Romanova and M. Hunger, *J. Phys. Chem. C*, 2008, **112**, 3811–3818.
51 D. Freude, M. Hunger, H. Pfeifer and W. Schwieger, *Chem. Phys. Lett.*, 1986, **128**, 62–66.
52 G. Engelhardt, H. G. Jerschkewitz, U. Lohse, P. Sarv, A. Samoson and E. Lippmaa, *Zeolites*, 1987, **7**, 289–292.
53 G. R. Goward, M. F. H. Schuster, D. Sebastiani, I. Schnell and H. W. Spiess, *J. Phys. Chem. B*, 2002, **106**, 9322–9334.
54 M. McCormick, R. N. Smith, R. Graf, C. J. Barrett, L. Reven and H. W. Spiess, *Macromolecules*, 2003, **36**, 3616–3625.